

Effect of Tag Dispersion On Fast ASL Methods

G. R. Lee¹, L. Hernandez-Garcia¹, D. Noll²

¹Biomedical Engineering, University of Michigan, Ann Arbor, MI, United States, ²University of Michigan, Ann Arbor, MI, United States

Introduction

Models for quantifying perfusion with continuous arterial spin labeling (CASL) techniques usually neglect dispersion of the tag during transit to the imaging region. Dispersion of the tag delivery function typically causes a modest change in the shape of the ASL signal timecourse for traditional ASL acquisitions. Turbo ASL acquisitions, on the other hand, apply shorter tagging durations and TRs to speed data acquisition. The shorter tag allows control image acquisition before the tag has arrived at the imaging slice. The tag image is then acquired the following TR after tag has had time to arrive. These sequences have been shown to be highly sensitive to transit time [1]. Thus, the presence of a spread of transit times due to dispersion of the bolus of tag is likely to significantly alter the shape of the turbo-CASL signal curve and affect flow quantification.

Theory

Following the formulation of Buxton et al., the ASL signal can be expressed as the convolution of a tag delivery function, $c(t)$, with exponential decay and residue functions [2]. The delivery function denotes when tag arrives at the imaging slice. For turbo-ASL this is the following TR from when spins were being inverted at the labeling plane. Some previous simulation work has been done in considering dispersion of the tag arrival function [2,3]. Analytical solutions for arrival functions blurred by either a Gaussian or uniform probability density function (PDF) have been computed previously for the case of a single rect (boxcar) labeling function [3]. To be of use for fMRI with turbo-CASL, this solution must be modified to take into account a periodic labeling function as used in fMRI experiments where the bolus from a given tagging interval is not necessarily fully spent by the time of the next tagging interval. In addition, image acquisition at the tagging plane tends to destroy the tag that has built up in the slice. This can be taken into account by breaking up the blurred tag arrival function into piecewise segments corresponding to each imaging interval (TR) and performing the convolution with the decay and residue functions on each piece individually. An analytical solution with this modification was given previously for non-dispersed tag arrival [1].

A drawback of Gaussian dispersion of the delivery function is the implication that some amount of tag arrived before labeling began due to the infinite temporal width of the Gaussian PDF. For the purposes of this work a dispersion function in the form of a Rayleigh PDF was assumed as it has a finite starting time. The parameter β characterizes the time to peak of the Rayleigh PDF. The delivery functions for periodic rect and Rayleigh dispersed arrivals for CASL are given by:

$$c_1(t) = \sum_{n=0}^{N-1} \text{rect}[(t - \Delta t - 2nTR) / \tau], \quad c_2(t) = c_1(t - \beta) \otimes \left[\frac{t}{\beta^2} e^{-t/(2\beta^2)} \cdot e^{t/T1_a} H(t) \right]$$

where Δt =transit time, τ =tag duration, $T1_a$ =arterial $T1$, \otimes represents convolution, and $H(t)$ is the Heaviside step function. In the second equation, the shift in $c_1(t)$ by β is to keep the bolus peak centered at the same location as in the rect case. The period of $c_1(t)$ is $2 \cdot TR$ reflecting the fact that spin labeling is applied only on alternate TRs in ASL acquisitions. The exponential decay with $T1_a$ is to account for the difference in decay for different arrival times. The dot-dash and dotted lines in Fig. 1 correspond to $c_1(t)$ and $c_2(t)$ respectively while the green and blue lines represent the corresponding ASL signal timecourses. To speed data fitting, analytical rather than numerical solutions for the ASL signal were obtained using Mathematica.

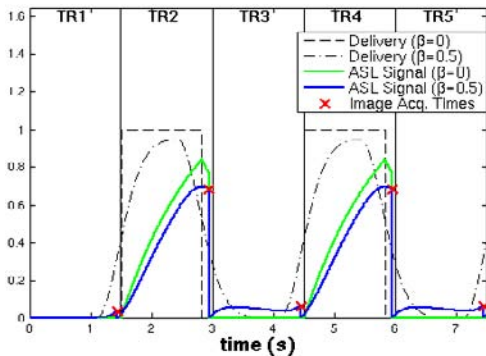


FIG. 1

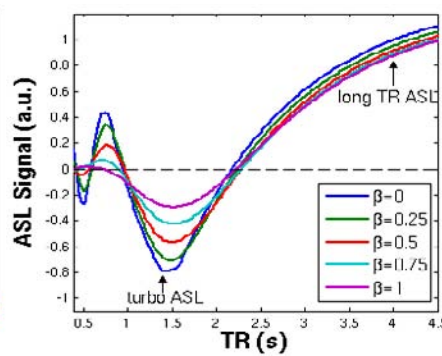


FIG. 2

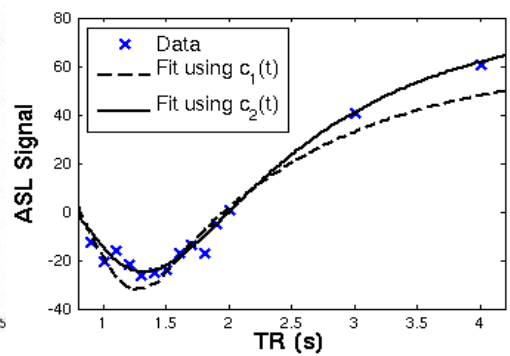


FIG. 3

Results and Discussion

In the simulation of Fig. 2, ASL signal is plotted vs TR when $\tau = TR - 150$ ms for a range of dispersions. It can be seen that the amplitude of the turbo-ASL signal is greatly attenuated as β becomes larger while the long TR signal is affected to a much lesser extent. The location of the turbo-CASL signal peak remains the same for all levels of dispersion. For all simulations, it was assumed $T1_{brain} = 1.35$ s, $T1_a = 1.65$ s, $\Delta t = 1.5$ s.

One human subject was scanned in accordance with University of Michigan IRB protocols. A two-coil turbo-CASL acquisition was performed for 12 equally spaced TR values between 0.9 and 2 s as well as two longer TRs of 3 and 4 s. Flow spoiling gradients ($b = 4$ s/mm²) were used to suppress contributions from large arteries. Three-parameter fits (Δt , CBF, β) of the data were performed with in Matlab using the analytical expressions for the ASL signal obtained from Mathematica. Fig. 3 shows a representative voxel from human subject data where the fit is greatly improved when dispersion is accounted for. The voxel chosen for display had a slightly larger dispersion value ($\beta = 0.64$) than average so that the difference in fits would be readily apparent. The average fitted value of β over all gray matter voxels was 0.56 ± 0.24 resulting in an average mean-squared error reduction of 20.4% in the data fits as compared to the case with no dispersion. The average β of 0.56 corresponds to a FWHM of 0.89 s for the Rayleigh dispersion kernel. There was a corresponding increase of 15.6% in the flow estimate, indicating that quantification is strongly affected by dispersion. Neglecting dispersion of the delivery function will result in underestimation of the true flow value. These preliminary results indicate that the dispersion of the delivery function is significant and should not be neglected during quantification of turbo-CASL and, to a lesser extent, long TR CASL data.

References: 1. Hernandez-Garcia *et al*, MRM 51 p.577 (2004) 2. Buxton *et al*, MRM 40 p. 383 (1998) 3. Hrabe *et al*, JMR 167 p. 49 (2004)

Support: NIH grant R01EB004346-01